



# pH-Dependent Conformational Analysis of Threonine Using Different Molecular Modeling Methods

Mikhail E. Kuznetsov<sup>1</sup> , Maria G. Khrenova<sup>1</sup> , Anna M. Kulakova<sup>1</sup> 

© The Authors 2026. This paper is published with open access at SuperFri.org

Conformational landscape of flexible molecules plays an important role in their reactivity, physicochemical properties and biological functions. The article presents a comparative study of the conformational stability of three protonated forms of threonine (Thr<sup>(+)</sup>, Thr<sup>(0)</sup>, Thr<sup>(-)</sup>) in aqueous solution using classical molecular dynamics (MD), umbrella sampling (US) and metadynamics (MTD) methods. It is shown that classical molecular dynamics fails to achieve ergodic sampling for Thr<sup>(0)</sup> and Thr<sup>(-)</sup> due to high rotational energy barriers around the C<sub>α</sub>-C<sub>β</sub> bond. The US method, despite being slightly more computationally expensive than classical MD, provides the most accurate Gibbs free energy profiles with minimal statistical error. Conventional MTD exhibits an unacceptably high confidence interval (up to 6 kcal/mol), while well-tempered MTD (WT-MTD) yields results that are quantitatively consistent with US (difference less than 0.2 kcal/mol) and an acceptable error margin (~1 kcal/mol). It was established that at pH < 9.62 (Thr<sup>(0)</sup> and Thr<sup>(+)</sup> forms), the trans conformation is the most stable, whereas for the deprotonated Thr<sup>(-)</sup> form, the gauche<sup>(-)</sup> conformation is preferred. At the same time, the energy differences between the conformers are small (1–2 kcal/mol), and the transition barriers vary within the range of 3–12 kcal/mol.

*Keywords: molecular dynamics, threonine, conformers, NAMD3.*

## Introduction

The physicochemical properties of molecules can be strongly influenced by their conformational composition, such as acidity/basicity [11] and circular dichroism spectra [10]. Also, in biological processes, certain conformations of active molecules are required for the process to occur. In this work, we investigated the conformations of  $\alpha$ -amino acid L-threonine under different pH conditions. This amino acid participates in post-translational modifications and is frequently found in active sites of enzymes. Conformational lability of threonine not only contributes to the tertiary structure stability, but can directly modulate catalytic activity, substrate recognition, and allosteric regulation [16].

Experimental approaches for assessing the relative stability of conformers are applicable to solid [4], gaseous [1], and liquid states [14] of molecules; however, evaluation in aqueous solution or within a protein complex at different pH remains challenging. Numerous computational methods exist for estimating the energies of individual molecular conformations in solution employing descriptions of the system at either quantum or classical molecular mechanics level. Quantum chemistry methods assume solving the Schrödinger equation numerically, which allows us to calculate the relative internal energies of different conformations. Further vibrational analysis provides a way to estimate the Gibbs free energy formally. Molecular mechanics methods, by contrast, treat atoms in molecules as charged spheres connected by springs, with interactions defined strictly by the force field.

In order to evaluate the energy of conformers in solution with explicit solvent molecules, it is necessary to either generate and evaluate a vast number of different configurations or to simulate a trajectory using molecular dynamics with forces derived from either quantum mechanics or molecular mechanics. Quantum calculations are much more computationally intensive, and

<sup>1</sup>Lomonosov Moscow State University, Moscow, Russia

molecular mechanics can be applied to this problem because no chemical bonds are broken or formed during conformational transitions. Therefore, in this study, we perform molecular dynamics simulations using a classical force field to estimate relative Gibbs free energy of stable conformations of threonine at different pH.

The article is organized as follows. Section 1 describes the molecular systems studied and details the computational setup for classical molecular dynamics, umbrella sampling, and metadynamics simulations. Section 2 presents the results obtained by each method, including the analysis of conformational populations, Gibbs free energy profiles, and a comparison of their computational efficiency. Finally, the Conclusion summarizes the key findings, compares the accuracy of the employed techniques, and provides recommendations for choosing the optimal enhanced sampling method for conformational analysis of flexible molecules in solution.

## 1. Methods

### 1.1. Molecular Systems

In aqueous solutions, the threonine molecule can exist in three protonation states (Fig. 1), as it contains two ionizable groups: an amino group with  $pK_a = 9.62$  and a carboxyl group with  $pK_a = 2.11$ . Thus, the molecule can adopt predominately a protonated form ( $\text{Thr}^{(+)}$ ) at  $\text{pH} < 2.11$ , a zwitterionic form ( $\text{Thr}^{(0)}$ ) at  $2.11 < \text{pH} < 9.62$ , and a deprotonated form ( $\text{Thr}^{(-)}$ ) at  $\text{pH} > 9.62$ . Each of these forms has three possible conformations, depending on the value of  $CC_\alpha C_\beta C_\gamma$  dihedral, that determines rotation around a single  $C_\alpha-C_\beta$  bond. These conformations are called  $\text{gauche}^{(-)}$ , trans and  $\text{gauche}^{(+)}$  (Fig. 2).

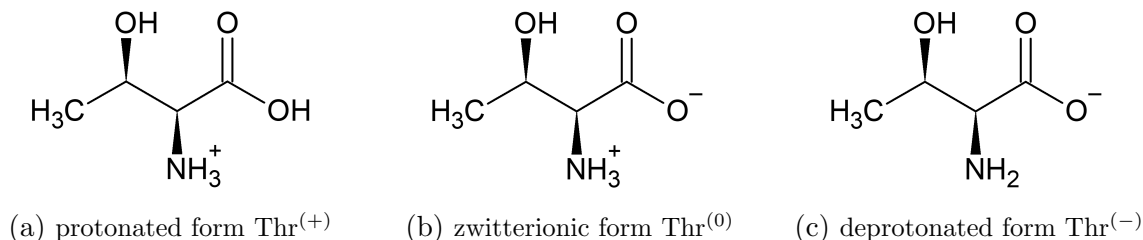


**Figure 1.** Structural formulas of L-threonine in different protonation states

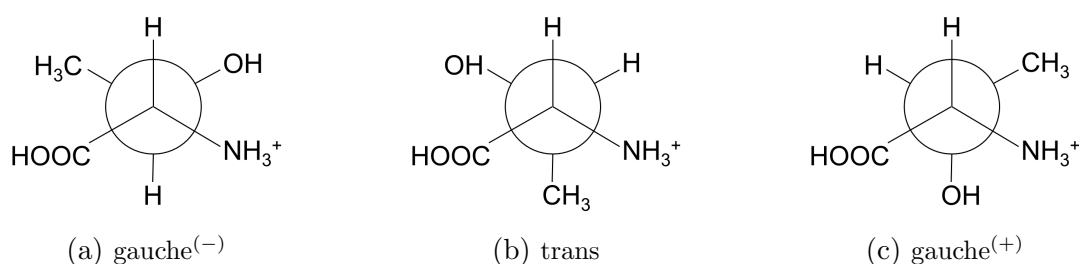


**Figure 2.** Newman projections showing conformations of the protonated form of L-threonine

Molecular model of threonine zwitterionic form at a neutral pH ( $\text{Thr}^{(0)}$ ) was created using the Discovery Studio software and pre-optimized. Two other forms of threonine, protonated ( $\text{Thr}^{(+)}$ , at low pH) and deprotonated ( $\text{Thr}^{(-)}$ , at high pH), were obtained from the zwitterionic form by adding or removing hydrogen atoms. The optimized geometries of  $\text{Thr}^{(+)}$ ,  $\text{Thr}^{(0)}$  and  $\text{Thr}^{(-)}$  were calculated using density functional theory (DFT) with the B3LYP functional [5]

and the 6-31G\*\* basis set [6], using the conductor-like polarizable continuum model (CPCM) [2] in ORCA 5.0.4 [12].

All three optimized forms of threonine were solvated in a rectangular water box and properly neutralized. The size of the water box was selected so that the distance between any atom of threonine and the cell border exceeded 12 Å. Sodium cations (for Thr<sup>(-)</sup>) or chlorine anions (for Thr<sup>(+)</sup>) were added to model systems for electroneutrality. The preparation of full atomic models, as well as the visualization and analysis of structures, was carried out using the VMD program [8].

Then, the structures were minimized using the steepest descent algorithm for 1000 steps. To relax the solvation shell, 0.5 ns classical molecular dynamics (MD) simulations with fixed threonine atoms were performed for all model systems. MD calculations were carried out in the NPT ensemble with a Langevin thermostat at 298 K and a Berendsen barostat at 1 atmosphere with 1 fs integration step. CHARMM36 force field [3] was used for threonine, and TIP3P for water [9]. Minimization, solvation shell relaxation and further molecular dynamics and metadynamics calculations were carried out using the NAMD3 software [13].

## 1.2. Classical Molecular Dynamics Simulations

For each of the three forms of threonine 500 ns molecular dynamics trajectories were calculated in the NPT ensemble. The parameters for the molecular dynamics simulation are similar to those used for solvation shell relaxation. Trajectory analysis allowed us to estimate the populations of the gauche<sup>(+)</sup>, gauche<sup>(-)</sup> and trans conformations for each form of threonine. Assuming that the resulting trajectories are ergodic, we can determine the relative energies of these conformations based on the Gibbs distribution using the following formula:  $\Delta\Delta G = \Delta G_1 - \Delta G_2 = -kT \ln\left(\frac{N_1}{N_2}\right)$ , where  $N_1$  and  $N_2$  are the number of MD frames of corresponding conformation.

## 1.3. Umbrella Sampling Simulations

For molecular dynamics simulations using the umbrella sampling method, four starting structures were prepared for each form of threonine. In these structures dihedral angle  $H_\alpha C_\alpha C_\beta H_\beta$  was constrained to values 0°, 100°, -100° and 180°. Preparation involved the direct modification of  $H_\alpha C_\alpha C_\beta H_\beta$  angle followed by energy minimization as described above.

Umbrella sampling simulations were also performed using the NAMD3 software package with the same MD parameters. The dihedral angle  $H_\alpha C_\alpha C_\beta H_\beta$  was selected as a collective variable with a harmonic biasing potential (force constant  $k = 0.01\text{--}0.03 \text{ kcal}\cdot\text{mol}^{-1}\cdot\text{deg}^{-2}$ ) applied along. The center of the biasing potential was systematically shifted from -180° to 160° in 20° increments. For each window, a MD trajectory of 10 ns was computed. To enhance the overlap of probability distributions for subsequent free energy analysis, additional simulations were performed with biasing potential centered at  $\pm 10^\circ$  and  $\pm 130^\circ$ .

Weighted histogram analysis method [15] (WHAM) was utilized to reconstruct Gibbs free energy profiles from statistical analysis of  $H_\alpha C_\alpha C_\beta H_\beta$  dihedral angle distributions in the umbrella sampling trajectories. In the WHAM program a value of  $10^{-4} \text{ kcal/mol}$  was used as the energy convergence criterion.

## 1.4. Metadynamics Simulations

For metadynamics (MTD) calculation the same collective variable ( $H_\alpha C_\alpha C_\beta H_\beta$  dihedral angle) was used. All metadynamics (MTD) trajectories were started from value of dihedral angles  $-100^\circ$ . Gaussian biasing potentials with initial Gaussian width (at half-height) of  $1^\circ$  and Gaussian height of  $1 \text{ kcal}\cdot\text{mol}^{-1}\cdot\text{deg}^{-2}$  were applied. New Gaussians were added every 100 integration steps. A total of ten independent 10 ns metadynamics trajectories were calculated for each of three threonine forms. A bias temperature of 1700 K was selected based on preliminary simulations testing various parameter values.

## 2. Results and Discussion

### 2.1. Classical Molecular Dynamics Simulations

One of the simplest methods to estimate the relative stability of molecule conformation is based on the Gibbs free energy distribution. This method requires to determine gauche<sup>(+)</sup>, gauche<sup>(-)</sup> and trans conformer population as the number of frames with each conformation. We calculated  $H_\alpha C_\alpha C_\beta H_\beta$  dihedral angle at each frame of MD trajectory and determined the corresponding conformation from its value.  $H_\alpha C_\alpha C_\beta H_\beta$  value between  $-120^\circ$  and  $0^\circ$  corresponds to trans conformation. If dihedral angle ranges from  $0^\circ$  to  $120^\circ$ , we are dealing with a gauche<sup>(+)</sup> conformation. The ranges from  $-180^\circ$  to  $-120^\circ$  and from  $120^\circ$  to  $180^\circ$  correspond to the gauche<sup>(-)</sup> conformation of threonine.

The  $H_\alpha C_\alpha C_\beta H_\beta$  distribution was investigated for all three forms of threonine at different pH values (Fig. 3). Despite several different calculations of molecular dynamic modeling for systems with high (Thr<sup>(-)</sup>) and neutral (Thr<sup>(0)</sup>) pH, which started from different initial conformations, it was not possible to obtain an ergodic trajectory. The systems were unable to overcome the high rotational energy barrier. As a result, it is impossible to determine the relative populations for Thr<sup>(-)</sup> and Thr<sup>(0)</sup>. In contrast, all three conformations were observed for the Thr<sup>(+)</sup> form, indicating lower rotational barriers. The relative Gibbs free energy was estimated using the energy of the most stable trans conformation as the zero reference point. The results are summarized in Tab. 1.

**Table 1.** Population and relative Gibbs free energy of Thr<sup>(+)</sup> conformations from classical molecular dynamics simulations

Conformation	$H_\alpha C_\alpha C_\beta H_\beta$ dihedral angle, deg	Number of frames	Population, %	$\Delta\Delta G$ kcal/mol
gauche <sup>(-)</sup>	$(-180, -120) \cup (120, 180)$	5217	26.1	0.30
trans	$(-120, 0)$	8628	43.1	0
gauche <sup>(+)</sup>	$(0, 120)$	6155	30.8	0.20

All molecular dynamics simulations were performed using NAMD3 software [13] compiled with GPU acceleration. The primary production runs were carried out using Tesla V100-SXM3-32GB. On this datacenter-grade GPU, the simulation of a small system ( $\sim 2000$  atoms) achieved a performance rate of 0.000500535 seconds per step, corresponding to an impressive throughput of approximately 172.6 ns per day. For each of three systems (Thr<sup>(+)</sup>, Thr<sup>(0)</sup> and Thr<sup>(-)</sup>), five independent 100 ns trajectories were generated, resulting in a total simulated time of 1.5  $\mu\text{s}$

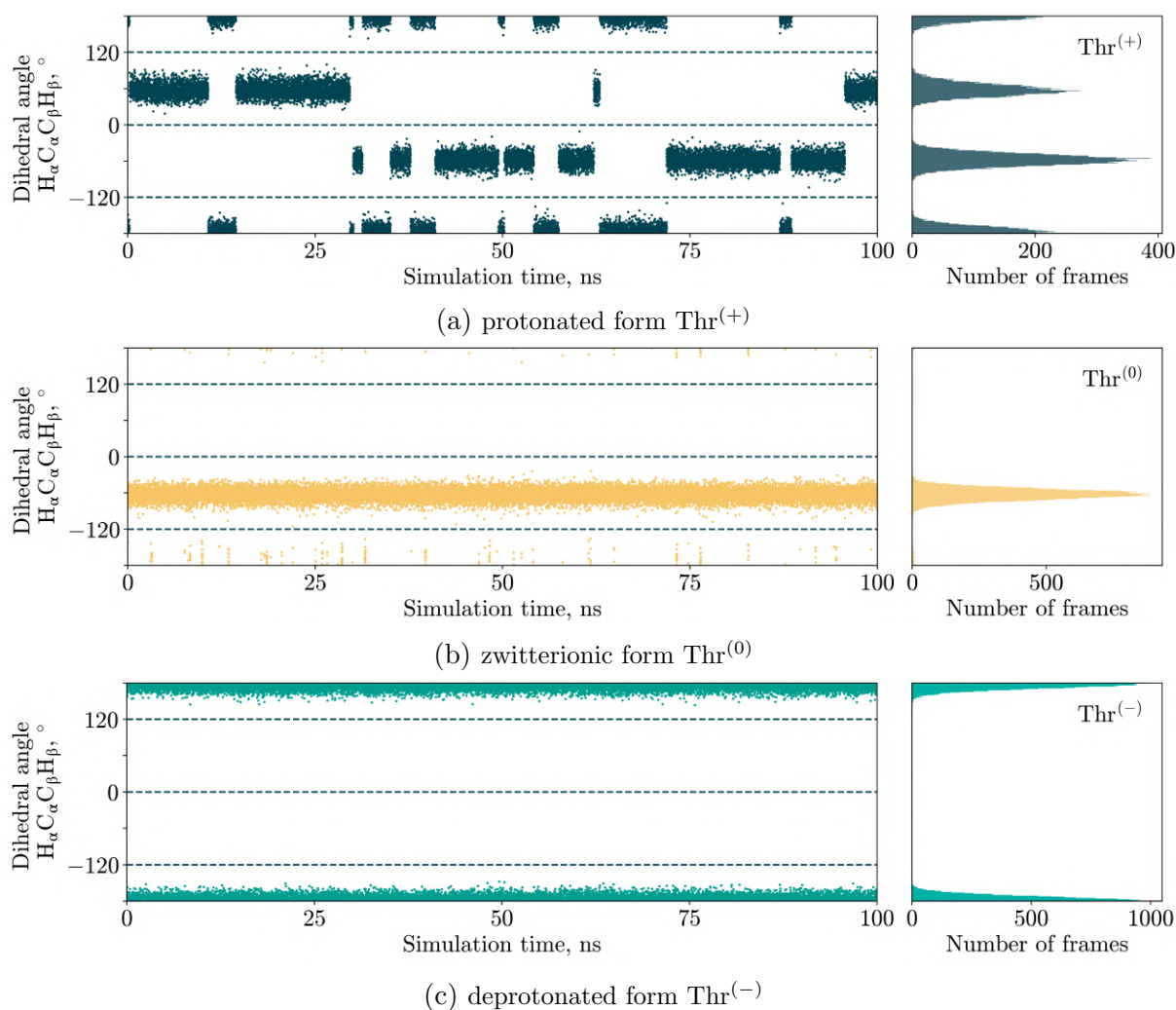


**Figure 3.**  $H_{\alpha}C_{\alpha}C_{\beta}H_{\beta}$  dihedral angle distribution during classical MD simulations

(500 ns per system). The cumulative computational time required to complete all 15 individual runs amounted to approximately 8.7 days of continuous GPU runtime.

## 2.2. Umbrella Sampling Simulations

After performing umbrella sampling molecular dynamics with bias potential ( $k = 0.01 \text{ kcal}\cdot\text{mol}^{-1}\cdot\text{deg}^{-2}$ ) centered at  $H_{\alpha}C_{\alpha}C_{\beta}H_{\beta}$  values from  $-180^{\circ}$  to  $160^{\circ}$  with  $20^{\circ}$  increments, the overlap of the  $H_{\alpha}C_{\alpha}C_{\beta}H_{\beta}$  distributions was checked. To achieve optimal overlap for the Thr<sup>(-)</sup> distributions, two additional MD trajectories with bias potential centered at  $10^{\circ}$  and  $-10^{\circ}$  were calculated. The force constants  $k$  were increased to  $0.03 \text{ kcal}\cdot\text{mol}^{-1}\cdot\text{deg}^{-2}$  for MD trajectories with bias potential centered at  $0^{\circ}$  and  $\pm 10^{\circ}$ . For bias potential centered at  $\pm 20^{\circ}$ ,  $\pm 100^{\circ}$ ,  $\pm 120^{\circ}$ , and  $\pm 140^{\circ}$  force constants were increased to  $0.02 \text{ kcal}\cdot\text{mol}^{-1}\cdot\text{deg}^{-2}$ . To achieve optimal overlap for the neutral form Thr<sup>(0)</sup> distributions, three additional MD trajectories with bias potential centered at  $130^{\circ}$ ,  $10^{\circ}$  and  $-10^{\circ}$  were calculated. The force constants  $k$  were increased to  $0.02 \text{ kcal}\cdot\text{mol}^{-1}\cdot\text{deg}^{-2}$  for MD trajectories with bias potential centered at  $0^{\circ}$  and  $\pm 10^{\circ}$ ,  $130^{\circ}$ . For Thr<sup>(+)</sup> simulations only force constants  $k$  were increased to  $0.02 \text{ kcal}\cdot\text{mol}^{-1}\cdot\text{deg}^{-2}$  for MD trajectories with bias potential centered at  $0^{\circ}$ ,  $\pm 20^{\circ}$ ,  $\pm 100^{\circ}$ ,  $\pm 120^{\circ}$ , and  $\pm 140^{\circ}$ . Since the obtained distributions of the dihedral angle overlap well with each

other (Fig. 4), it is possible to calculate Gibbs free energy profiles using the weighted histogram analysis method (Fig. 5).

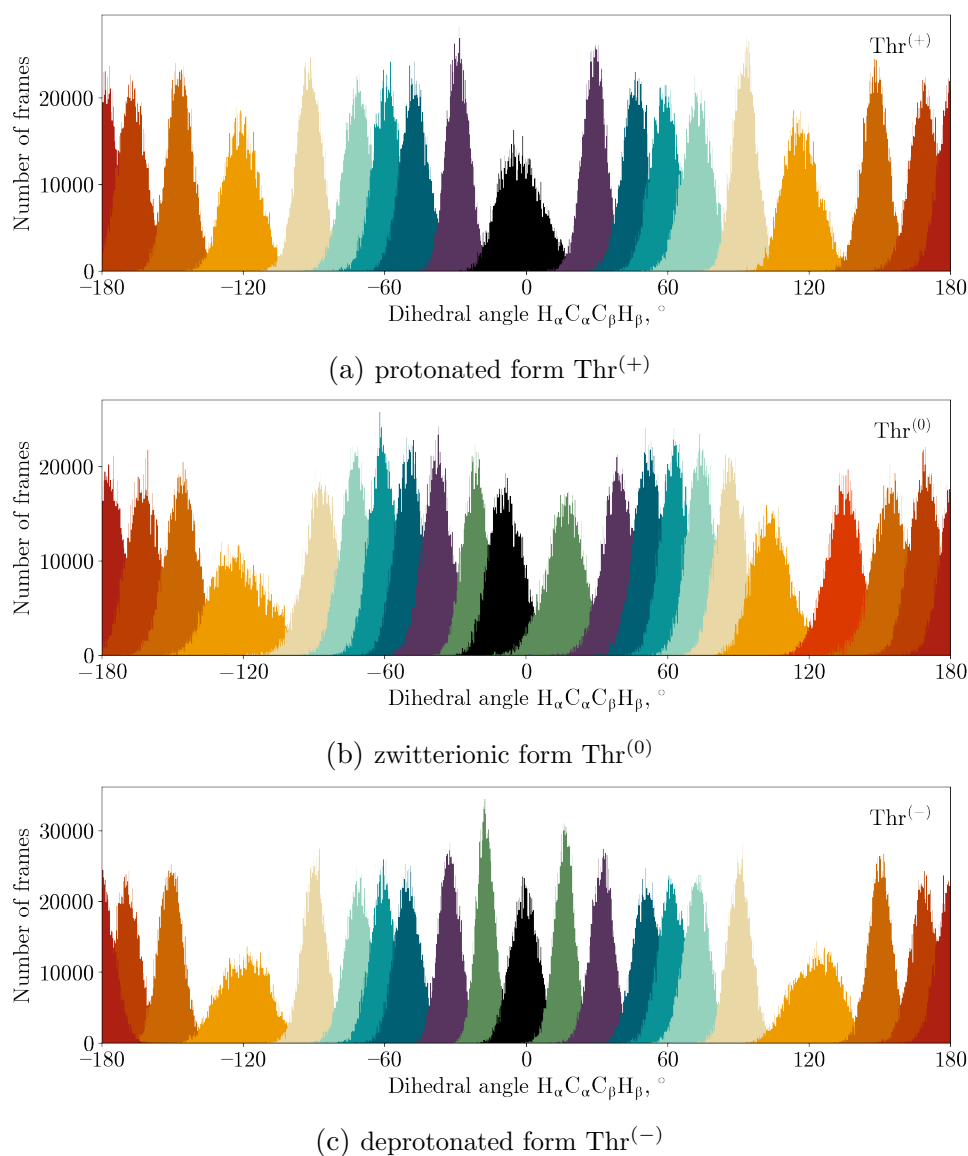


**Figure 4.** Distribution of  $H_{\alpha}C_{\alpha}C_{\beta}H_{\beta}$  dihedral angle distributions during umbrella sampling simulations

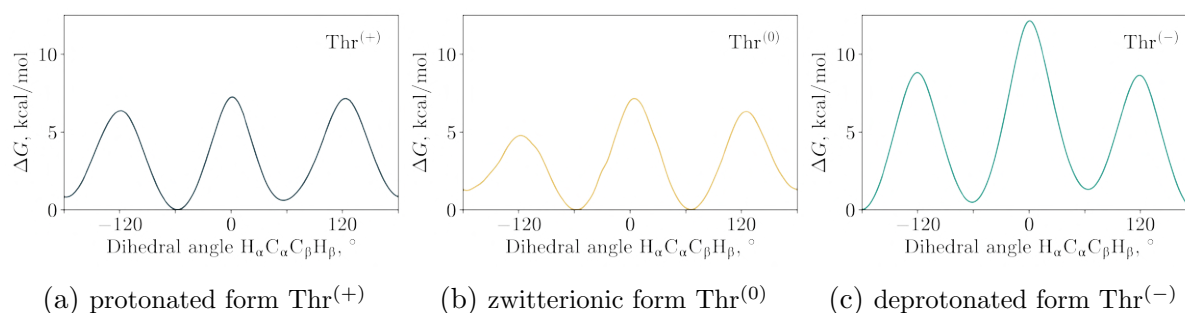


**Figure 5.** The Gibbs free energy  $C_{\alpha}-C_{\beta}$  rotation profiles calculated by umbrella sampling and WHAM methods

The results obtained by the classical molecular dynamics method (Tab. 1) are in good agreement with the results of the umbrella sampling (Tab. 2) for Thr<sup>(+)</sup> form. The trans-conformation turned out to be the most stable, while the gauche<sup>(-)</sup> conformation is less stable than the gauche<sup>(+)</sup> one. In addition, it was observed that the rotation barriers for the deprotonated and zwitterionic forms are on average higher than for the protonated ones. This explains why conformations do not change into each other in classical molecular dynamics. The data obtained also confirm that in the Thr<sup>(0)</sup> form the rotation barrier from the gauche<sup>(-)</sup> to the trans conformation is small (2.5 kcal/mol). As a result, classical molecular dynamics quickly leaves the gauche<sup>(-)</sup> conformation and transforms into a trans conformation. Nevertheless, the molecules sometimes return to the gauche<sup>(+)</sup> conformation, although the energy barrier for this transition is lower than for the transition from trans to gauche<sup>(-)</sup> conformation.

**Table 2.** Relative Gibbs free energy of threonine conformations calculated by umbrella sampling and WHAM methods

Conformation	$H_{\alpha}C_{\alpha}C_{\beta}H_{\beta}$ dihedral angle, deg	$\Delta\Delta G$ , kcal/mol		
		Thr <sup>(+)</sup>	Thr <sup>(0)</sup>	Thr <sup>(-)</sup>
gauche <sup>(-)</sup>	$(-180, -120) \cup (120, 180)$	0.8	2.6	0.0
trans	$(-120, 0)$	0.0	0.0	0.5
gauche <sup>(+)</sup>	$(0, 120)$	0.6	1.9	1.3

For protonated and zwitterionic forms of threonine, trans conformer is the most stable. This is due to compensation of steric difficulties by electrostatic interactions between the -OH group, amino- and carboxyl groups. In the deprotonated form (Thr<sup>(-)</sup>), the electrostatic interaction with the carboxyl group weakens, which makes the gauche<sup>(-)</sup> conformer more stable.

In contrast to classical molecular dynamics simulations, the umbrella sampling method imposes an external biasing potential to constrain the system along the reaction coordinate, which leads to increased computational cost per step. On the Tesla V100-SXM3-32GB GPU, umbrella sampling simulations achieved a performance of 0.000690609 seconds per step, corresponding to a throughput of 125.107 ns/day – approximately 27.5% slower than classical MD runs on the same hardware. The umbrella sampling calculations were performed separately for each protonation state of threonine. Specifically, 19 independent biased simulations were conducted for Thr<sup>(+)</sup>, 22 for Thr<sup>(0)</sup>, and 21 for Thr<sup>(-)</sup>, each with a trajectory length of 10 ns. The cumulative computational time required to complete all umbrella sampling simulations was approximately 4.96 days of continuous GPU runtime.

### 2.3. Metadynamics Simulations

Gibbs free energy profiles were calculated from the metadynamics data using the parameters of the Gaussian potentials at timestep  $\tau$  ( $\sigma$  – Gaussian width,  $w$  – Gaussian height,  $\theta$  – value of  $H_{\alpha}C_{\alpha}C_{\beta}H_{\beta}$  dihedral angle) by the following formulas ( $\Delta T$  – bias temperature 1700 K):

$$\Delta G_{\text{MTD}}(\theta) = -w \sum_{\substack{n=1 \\ \tau=n\tau_G}} \exp\left(-\frac{(\theta - \theta(\tau))^2}{2\sigma^2}\right),$$

$$\Delta G_{\text{WT-MTD}}(\theta, \Delta T) = -\frac{T + \Delta T}{\Delta T} \sum_{\substack{n=1 \\ \tau=n\tau_G}} w(\tau) \exp\left(-\frac{(\theta - \theta(\tau))^2}{2\sigma^2}\right).$$

Data were additionally referred to the minima of Gibbs free energy. To estimate the spread of values, we used data obtained from ten different metadynamic (MTD) and ten well-tempered metadynamics (WT-MTD) trajectories. The variation in value was determined as the difference between the maximum and minimum values for each trajectory. The resulting intervals and the average profile are shown in Fig. 6.

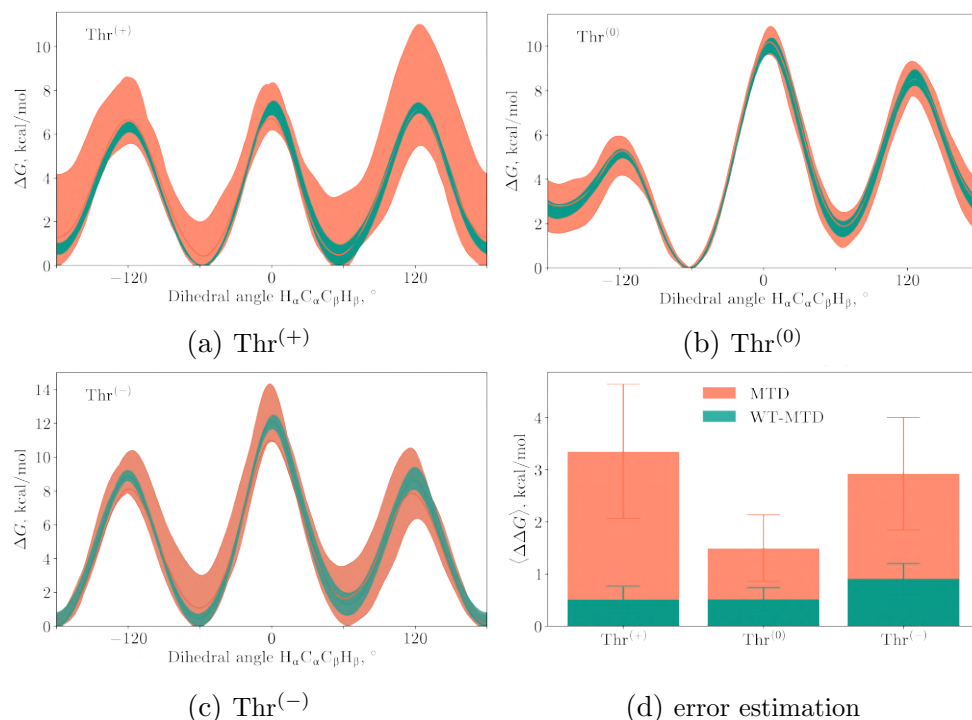


**Figure 6.** The Gibbs free energy  $C_\alpha$ - $C_\beta$  rotation profiles and error estimation calculated using metadynamics (MTD) and well-tempered metadynamics (WT-MTD)

Analysis of the obtained data shows that the metadynamics (MTD) gives significant deviations in the profile values, reaching 6 kcal/mol. At the same time, the deviations for the profiles obtained using the WT-MTD method do not exceed 1.5 kcal/mol. The energies of stable conformations for each of the forms were determined similarly to the US results using profiles obtained by the WT-MTD method (Tab. 3).

**Table 3.** Relative Gibbs free energy of threonine conformations calculated by well-tempered metadynamics

Conformation	$H_\alpha C_\alpha C_\beta H_\beta$ dihedral angle, deg	$\Delta\Delta G$ , kcal/mol		
		$\text{Thr}^{(+)}$	$\text{Thr}^{(0)}$	$\text{Thr}^{(-)}$
gauche <sup>(-)</sup>	$(-180, -120) \cup (120, 180)$	$0.8 \pm 0.2$	$2.8 \pm 0.2$	0.0
trans	$(-120, 0)$	0.0	0.0	$0.3 \pm 0.2$
gauche <sup>(+)</sup>	$(0, 120)$	$0.6 \pm 0.3$	$2.0 \pm 0.2$	$1.0 \pm 0.5$

The relative Gibbs free energy values of threonine conformations, obtained by umbrella sampling and well-tempered metadynamics methods, are close to each other. The difference between them is less than 0.2 kcal/mol, which is comparable to the spread of values obtained in the WT-MTD series of calculations.

Metadynamics and well-tempered metadynamics simulations exhibited nearly identical computational performance, as both methods differ from classical molecular dynamics primarily in the periodic deposition of Gaussian bias potentials every 100 simulation steps. On the Tesla V100-SXM3-32GB GPU, the average performance for both metadynamics variants was 0.000572646 seconds per step, corresponding to a throughput of 150.879 ns/day. For each protonation state of threonine, ten independent metadynamics and ten independent well-tempered metadynamics simulations were performed, each with a trajectory length of 10 ns. The cumulative computational time required to complete all metadynamics and well-tempered metadynamics simulations was approximately 3.98 days of continuous GPU runtime.

## 2.4. Comparison of Methods

The relative Gibbs free energies calculated in this work using classical molecular dynamics, umbrella sampling with WHAM, and metadynamics are in good agreement with each other. All methods employed in this study utilized the CHARMM force field for model description. In the literature, there are articles where the threonine molecule is described using quantum-chemical methods.

In Ref. [14], various conformations of threonine in aqueous solution were investigated using the MP2, B3LYP/6-31G\*\*++, and M062X/6-31G\*\*++ methods, with the IEF-PCM implicit solvent model. A total of 88 conformations were identified, and for the most stable ones, a correlation with experimental data was established. In the experiments, solid samples and solutions of threonine were studied using vibrational circular dichroism, IR, and Raman spectroscopy. The authors demonstrate that: *gauche*<sup>(+)</sup> conformation is the most stable for Thr<sup>(+)</sup> and Thr<sup>(0)</sup>, *trans* conformation is preferred for Thr<sup>(-)</sup>. The energy differences within the MP2 framework between conformations range from 1.5 (*gauche*<sup>(+)</sup> and *gauche*<sup>(-)</sup> for Thr<sup>(+)</sup>) to 6.5 kcal/mol (*trans* and *gauche*<sup>(+)</sup> for Thr<sup>(-)</sup>).

In Ref. [7], the conformations of the zwitterionic form of threonine were studied with explicit solvent represented by 7 water molecules using the B3LYP/6-31G\*++ method. For the four most stable clusters, the authors observed agreement with experimental IR and Raman spectra. The most stable conformation for Thr<sup>(0)</sup> is *gauche*<sup>(-)</sup>, with an energy difference of 0.3 kcal/mol relative to *gauche*<sup>(+)</sup>, as for the gas phase neutral threonine [1].

Thus, the literature data formally exhibit rather poor agreement both among themselves and with the results obtained in this work, which can be attributed to several factors. Primarily, this discrepancy arises from the use of different methodologies: quantum-chemical methods, which describe electronic structure more accurately, and molecular mechanics methods, which capture dynamics and statistics on scales inaccessible to quantum approaches. Additionally, solvent representation differs, which may also contribute to the differences in energy. It should be noted that the obtained energy differences between conformations generally do not exceed 1–2 kcal/mol, which is comparable to the accuracy levels achievable by both quantum and classical methods.

Among the computational methods used in this study, classical molecular dynamics proved to be the most computationally efficient, achieving a throughput of 172.615 ns/day on one Tesla V100-SXM3-32GB GPU. However, despite its speed, classical MD is inherently limited by high energy barriers and cannot reliably determine transition free energies or complete conformational profiles, as it fails to ensure ergodic sampling of the entire conformational space within feasible simulation times. Umbrella sampling is approximately 27.5% slower than classical MD

and requires careful selection of a sufficient number of windows with adequate histogram overlap to ensure convergence. But US is relatively insensitive to simulation length per window and provides the most accurate Gibbs free energy profiles with negligible statistical error. In contrast, classical metadynamics exhibited unsatisfactory performance, yielding energy value scatter up to 6 kcal/mol – comparable to the barrier heights themselves and far exceeding the energy differences between stable conformations. Well-tempered metadynamics significantly improves upon standard MTD, achieving a throughput of 150.879 ns/day with an acceptable error margin of approximately 1 kcal/mol and quantitative agreement with US results. Despite its slightly higher computational cost, umbrella sampling remains the preferred method due to its superior accuracy and negligible statistical error compared to well-tempered metadynamics.

## Conclusion

Classical molecular dynamics simulations principally allow one to determine relative Gibbs free energies of stable conformations under the assumption of ergodicity of the performed simulations, but not energy barriers of transitions between conformations. In our particular system, transition energy barriers are high and, therefore, this condition cannot be achieved even with a 50-fold increase in trajectory simulation time relative to enhanced sampling methods.

Umbrella sampling enables calculation of the entire rotational free energy profile, including both energy barriers and relative energies of stable conformations. Among the methods employed in this work, it exhibits the lowest uncertainty, with negligible statistical error. Since the conformational coordinate in this work ( $H_\alpha C_\alpha C_\beta H_\beta$  dihedral angle) is well-defined, this method proves to be the least sensitive to reductions in simulation time.

Classical metadynamics yields unsatisfactory results: the uncertainty in energy values reaches up to 6 kcal/mol, which is comparable with the magnitude of the energy barriers and significantly exceeds the energy differences between stable conformations. Well-tempered metadynamics (WT-MTD) demonstrates an acceptable error margin of approximately 1 kcal/mol and shows quantitative agreement with US results; however, it requires careful parameterization of the applied bias potentials and bias temperature. Furthermore, WT-MTD should have longer trajectories and is characterized by greater uncertainty than umbrella sampling method.

US and WT-MTD methods demonstrate consistent results, showing that at pH values below 9.62, the trans conformation is the more stable form of threonine, whereas for the deprotonated form, the gauche<sup>(-)</sup> conformation is preferred. However, the relative energies of all conformations are close ( $\sim 1$ – $2$  kcal/mol), while the energy barriers show greater variation ( $\sim 3$ – $12$  kcal/mol).

## Acknowledgments

The work was conducted under the state assignment of Lomonosov MSU 121031300176-3. The research was carried out using the equipment of the shared research facilities of HPC computing resources at Lomonosov Moscow State University [17] including Istok computing system (Agreement 075-15-2025-541).

*This paper is distributed under the terms of the Creative Commons Attribution-Non Commercial 3.0 License which permits non-commercial use, reproduction and distribution of the work without further permission provided the original work is properly cited.*

## References

1. Alonso, J.L., Pérez, C., Sanz, M.E., *et al.*: Seven conformers of L-threonine in the gas phase: a LA-MB-FTMW study. *Physical Chemistry Chemical Physics* 11(4), 617–627 (2009). <https://doi.org/10.1039/b810940k>
2. Barone, V., Cossi, M.: Quantum calculation of molecular energies and energy gradients in solution by a conductor solvent model. *The Journal of Physical Chemistry A* 102(11), 1995–2001 (1998). <https://doi.org/10.1021/jp9716997>
3. Best, R.B., Zhu, X., Shim, J., *et al.*: Optimization of the additive CHARMM all-atom protein force field targeting improved sampling of the backbone  $\phi$ ,  $\psi$  and side-chain  $\chi_1$  and  $\chi_2$  dihedral angles. *Journal of Chemical Theory and Computation* 8(9), 3257–3273 (2012). <https://doi.org/10.1021/ct300400x>
4. Dubey, P., Mukhopadhyay, A., Viswanathan, K.S.: Do amino acids prefer only certain backbone structures? Steering through the conformational maze of l-threonine using matrix isolation infrared spectroscopy and ab initio studies. *Journal of Molecular Structure* 1175, 117–129 (2019). <https://doi.org/10.1016/j.molstruc.2018.07.066>
5. Hamprecht, F.A., Cohen, A.J., Tozer, D.J., Handy, N.C.: Development and assessment of new exchange-correlation functionals. *The Journal of Chemical Physics* 109(15), 6264–6271 (1998). <https://doi.org/10.1063/1.477267>
6. Hariharan, P.C., Pople, J.A.: The influence of polarization functions on molecular orbital hydrogenation energies. *Theoretica Chimica Acta* 28(3), 213–222 (1973). <https://doi.org/10.1007/BF00533485>
7. Hernández, B., Pflüger, F., Adenier, A., *et al.*: Energy maps, side chain conformational flexibility, and vibrational features of polar amino acids L-serine and L-threonine in aqueous environment. *The Journal of Chemical Physics* 135(5), 055101 (2011). <https://doi.org/10.1063/1.3617415>
8. Humphrey, W., Dalke, A., Schulten, K.: VMD: Visual Molecular Dynamics. *Journal of Molecular Graphics* 14(1), 33–38 (1996). [https://doi.org/10.1016/0263-7855\(96\)00018-5](https://doi.org/10.1016/0263-7855(96)00018-5)
9. Jorgensen, W.L., Chandrasekhar, J., Madura, J.D., *et al.*: Comparison of simple potential functions for simulating liquid water. *The Journal of Chemical Physics* 79(2), 926–935 (1983). <https://doi.org/10.1063/1.445869>
10. Kundrat, M.D., Autschbach, J.: Computational Modeling of the Optical Rotation of Amino Acids: A New Look at an Old Rule for pH Dependence of Optical Rotation. *Journal of the American Chemical Society* 130(13), 4404–4414 (2008). <https://doi.org/10.1021/ja0782571>
11. Lu, H., Chen, X., Zhan, C.G.: First-Principles Calculation of p Ka for Cocaine, Nicotine, Neurotransmitters, and Anilines in Aqueous Solution. *The Journal of Physical Chemistry B* 111(35), 10599–10605 (2007). <https://doi.org/10.1021/jp072917r>

12. Neese, F.: Software update: The ORCA program system–version 5.0. *Wiley Interdisciplinary Reviews: Computational Molecular Science* 12(5), e1606 (2022). <https://doi.org/10.1002/wcms.1606>
13. Phillips, J.C., Hardy, D.J., Maia, J.D.C., *et al.*: Scalable molecular dynamics on CPU and GPU architectures with NAMD. *The Journal of Chemical Physics* 153(4), 044130 (2020). <https://doi.org/10.1063/5.0014475>
14. Quesada-Moreno, M.M., Marquez-Garcia, A.A., Aviles-Moreno, J.R., *et al.*: Conformational landscape of l-threonine in neutral, acid and basic solutions from vibrational circular dichroism spectroscopy and quantum chemical calculations. *Tetrahedron: Asymmetry* 24(24), 1537–1547 (2013). <https://doi.org/10.1016/j.tetasy.2013.09.025>
15. Souaille, M., Roux, B.: Extension to the weighted histogram analysis method: combining umbrella sampling with free energy calculations. *Computer Physics Communications* 135(1), 40–57 (2001). [https://doi.org/10.1016/S0010-4655\(00\)00215-0](https://doi.org/10.1016/S0010-4655(00)00215-0)
16. Szidarovszky, T., Czakó, G., Császár, A.G.: Conformers of gaseous threonine. *Molecular Physics* 107(7), 761–775 (2009). <https://doi.org/10.1080/00268970802616350>
17. Voevodin, V.V., Antonov, A.S., Nikitenko, D.A., *et al.*: Supercomputer Lomonosov-2: Large Scale, Deep Monitoring and Fine Analytics for the User Community. *Supercomputing Frontiers and Innovations* 6(2), 4–11 (2019). <https://doi.org/10.14529/jsfi190201>